

Dielectric spectra of polythiophene nanoparticles synthesized at different magnetic flux densities

MERIH SERIN^{1,*}, SAHIN YAKUT^{2,*}, KEMAL ULUTAS², MURAT CALISKAN¹, DENIZ BOZOGLU², DENIZ DEGER², KEZIBAN HUNER³, FERDANE KARAMAN³

¹Department of Physics, Faculty of Arts and Sciences, Yildiz Technical University, 34220, Esenler/ Istanbul, Turkey

²Department of Physics, Faculty of Science, Istanbul University, 34134, Vezneciler, Istanbul, Turkey

³Department of Chemistry, Faculty of Arts and Science, Yildiz Technical University, 34220, Esenler, Istanbul, Turkey

Polythiophene nanoparticles successfully synthesized at different magnetic flux densities, which have values between 1,5 – 4,6 kGauss, were studied. The samples were prepared by dropping the dilute colloidal solutions of the PTh nanoparticles in pure water on the copper grids coated with carbon film. The sizes of polythiophene nanoparticles were determined by STEM analysis. It was observed that polythiophene nanoparticles were aggregated by the effect of magnetic flux. Dielectric measurements were performed using an impedance analyzer in the frequency range 0.1Hz-20MHz at room temperature. Three polarization mechanisms were detected. The AC conductivity obeys the Jonscher Law. The results obtained for polythiophene without and with magnetic flux effect were compared. It was observed that the presence of magnetic flux affects the structure of polythiophene by increasing the electrical capacitance at frequencies lower than 10^2 Hz and frequencies higher than 10^5 Hz. However, among the samples under the influence of magnetic flux, there isn't a remarkable difference with increasing flux density.

(Received December 2, 2021; accepted June 7, 2022)

Keywords: Polymer composite, Nanoparticles, Magnetic flux, Dielectric spectroscopy, AC conductivity

1. Introduction

Conjugated polymers exhibit conducting or semiconducting which may be suitable candidates because of their optical and electrical properties such as dielectric constant, refractive index, impedance, and permittivity. These parameters provide important information for optimization in technological applications such as chemical and optical sensors, light-emitting diodes and displays, photovoltaic devices, molecular devices, and DNA detection [1,2]. Among these polymers, polythiophenes are the most attractive because their electrical and physical properties can be easily modified to use as active materials for electrodes in supercapacitors, electricity, dissipative coatings, components of diodes and field-effect transistors, flexible electroluminescent lamps, solar cells, photochemical resists, nonlinear optic devices, batteries, and organic LEDs [3–7].

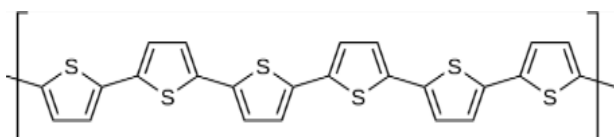


Fig. 1. Chemical structure of unsubstituted polythiophene

Unsubstituted polythiophene has a chain of alternating double and single bonds leading to π electron delocalization along the polymer backbone [8]. As seen in Fig.1, each first and fourth carbon atom is bonded with a sulfur atom to form

a thionyl ring. Another hand, the bond between the second and the third carbon atom has more single bond character than other bonds between C atoms [9]. In the literature, the conductivity of PTh synthesized with different polymerization techniques was studied. The room temperature conductivity of unsubstituted PTh prepared by chemical oxidative technique exhibited $3.2 \times 10^{-5} \Omega \cdot m$ [10]. The conductivity of PTh thin films synthesized by the chemical oxidative method was $10^{-5} \Omega \cdot m$ [11,12]. In another study, the conductivity of PTh which was measured in a nitrogen gas atmosphere at 318 K was found to be $7.2 \times 10^{-1} \Omega \cdot m$ [13].

In the synthesis of many polymers, the magnetic field effect has been investigated and it has been shown to increase the polymerization reaction rate and chain length [2,3,14,5–7,9–13]. However, there is no study examining the magnetic field effect on conductive polymers.

This study aims to investigate the dielectric properties of non-substituted polythiophene (PTh) nanoparticles, a semiconductor polymer, synthesized under different magnetic flux density fields (between 1,5 – 4,6 kGauss) applied and by chemical oxidative polymerization technique. As a result, based on the results of the frequency-dependent (the range of 0,1 Hz - 20 MHz) dielectric constant, dielectric loss, and AC conductivity, the effect of the magnetic field in the synthesis of PTh nanoparticles was investigated, and possible polarization regions in the structure were identified.

2. Experimental details

2.1. Materials and measurements

Thiophene (purity of 99%), poly (styrene sulfonic acid) (PSSA) (purity of 99%), and $\text{Cu}(\text{NO}_3)_2$ (purity of 99%) were purchased from Sigma-Aldrich. Hydrogen peroxide and hydrochloric acid were obtained from Prolabo France. All experiments were carried out under an inert atmosphere. Deionized water was used throughout the experiment. The electron microscope images of the samples were obtained by Philips XL30 ESEM-FEG/EDAX system using STEM (scanning transmission electron microscopy) technique with a boron detector. The samples were prepared by dropping the dilute colloidal solutions of the PTh nanoparticles in pure water on the copper grids coated with carbon film.

The sizes of PTh nanoparticles were determined in the range of 94 – 120 nm by STEM images. The dielectric spectroscopy measurements of polythiophene nanoparticles were performed by Alpha-A High-Resolution Dielectric, Conductivity and Impedance Analyzer (Novocontrol Technologies) in the frequency range 0.1 Hz - 20 MHz at room temperature. Frequency-dependent AC conduction results were derived from capacitance and dielectric loss factor ($\tan \delta$) results.

2.2. Preparation of polythiophene nanoparticles

Polythiophene nanoparticles were synthesized from chemical oxidative polymerization of thiophene by an oxidant/catalyst system of hydrogen peroxide/ $\text{Cu}(\text{NO}_3)_3$ in an aqueous medium under a nitrogen atmosphere with and without an external magnetic field. Poly (styrene sulfonic acid) was used as a dopant and dispersant. The details of the synthesis method were given elsewhere [14]. The abbreviations PTh-0, PTh-1.5, PTh-2.5, and PTh-4.6 were used for the samples synthesized under external magnetic flux densities of 0, 1.5, 2.5, and 4.6 k Gauss, respectively. After polymerization, the product was cleaned, for two weeks, using a dialysis membrane and dried at room temperature.

2.3. Dielectric spectroscopy measurements

For dielectric measurements, polythiophene nanoparticle samples were placed between two gold-plated brass electrodes. The ac signal frequency has been varied in a wide range of frequencies such as 0.1 Hz-20 MHz. The dielectric parameters of PTh such as capacitance (C), and loss tangent ($\tan \delta$) are measured as a function of frequency. Dielectric constant (K'), and ac conductivity values are calculated.

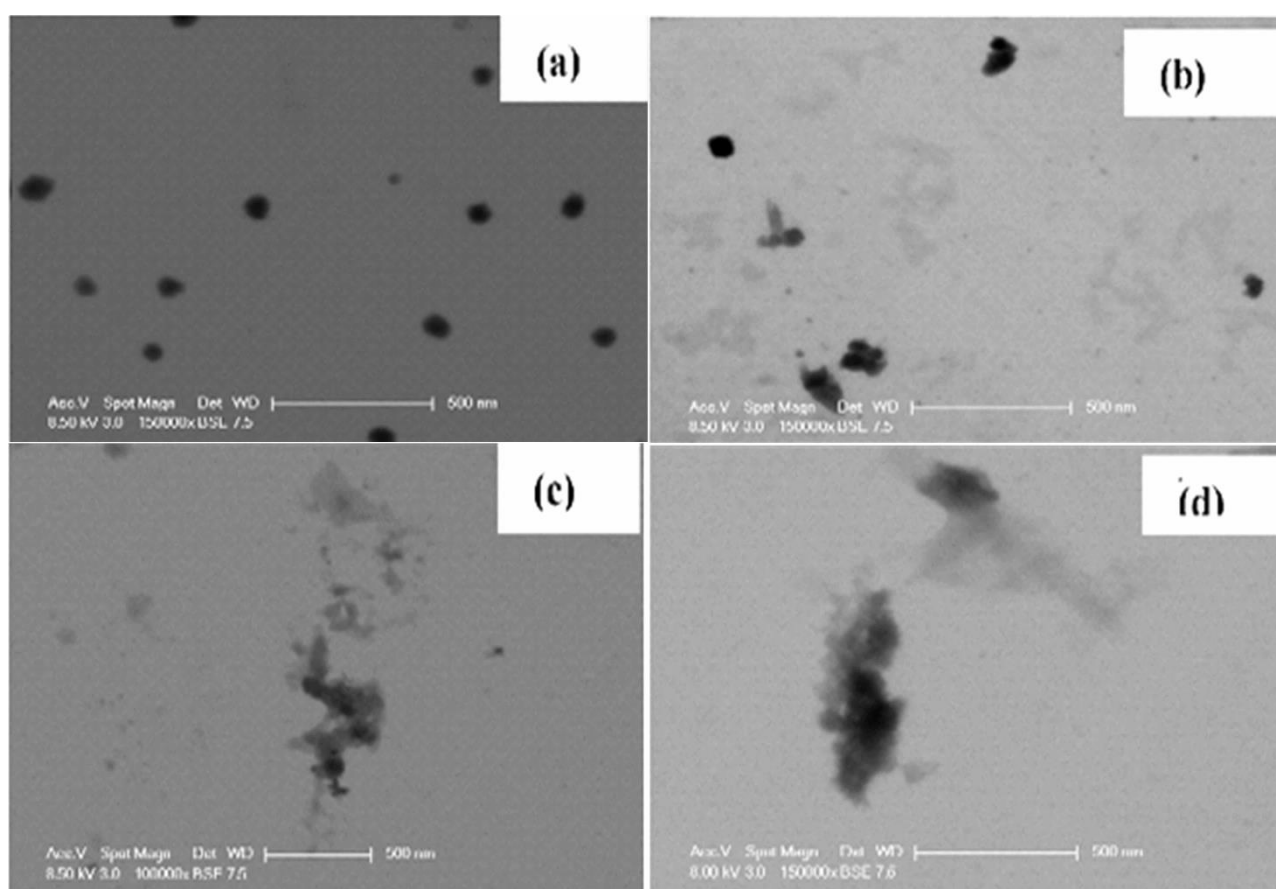


Fig. 2. STEM images of polythiophene nanoparticles synthesized under different magnetic fields (a) 0 kGauss (b) 1.5 kGauss (c) 2.5 kGauss (d) 4.6 kGauss

3. Results and discussions

3.1. Characterization of polythiophene nanoparticles

The hydrodynamic radii of nanoparticles were measured as 120 nm and 94 nm for the samples synthesized with and without a magnetic field, respectively, by the dynamic light scattering technique [14]. The morphologies of the particles were seen in the STEM images of the nanoparticles, given in Fig. 2. It looks like the sample synthesized without a magnetic field is stiffer than the samples synthesized under a magnetic field. It can be stated that the magnetic field considerably affects the aggregation of polythiophene chains. Aggregation of polythiophene chains causes softer samples.

3.2. Dielectric properties

Dielectric spectroscopy is a powerful measurement technique used to determine the dielectric properties of materials as a function of frequency. It is based on the calculation of values such as conductivity, capacitance, impedance, inductance, and admittance of the material as a result of the interaction of the electrical dipole moments of the materials with the electric field. It also provides information about many mechanisms such as polarization, electrical conductivity, dipole behavior, dielectric relaxation, and phase transitions in the material [15–20]. For dielectric materials with a wide variety of applications, dielectric characterization is required to have the desired values in terms of device design and performance. The variation of the dielectric constant with frequency is determined. The behavior of the real and imaginary parts of the dielectric constant can be related to the dielectric loss factor. Each polarization mechanism has different effects on the dielectric constant when its characteristic resonance frequency is exceeded. Besides, each of the polarization mechanisms causes dielectric loss ($\tan \delta$) at frequencies close to its resonant frequency.

The dielectric constant can be calculated using the parallel plate capacitor formula:

$$\kappa' = Cd/\epsilon_0 A \quad (1)$$

where d is the thickness of the sample, A is the surface area of electrodes, ϵ_0 is the electrical permittivity of vacuum and C is the capacitance of the sample [21].

3.2.1. Frequency dependence of dielectric constant of polythiophene nanoparticles

The frequency dependence of the dielectric constant of polythiophene nanoparticles synthesized at different magnetic fields is shown in Fig.3. It is observed that the dielectric constant (K') decreases with frequency. The high values of K' at the 1-100 Hz frequency region are attributed to the motions of the aggregates of PTh nanoparticles. The

aggregate can follow the applied field at low frequencies. As a result of this behavior, polarization increases toward low frequencies. Hence, increasing polarization lead to an increase in the dielectric constant of the sample [17]. As frequency increases, the aggregate cannot follow the applied field, and their contribution to total polarization decreases [22]. To analyze the behavior of the dielectric constant depending on frequency, the Cole-Cole equation can be used as shown in the equation below:

$$\epsilon^* - \epsilon_\infty / \Delta\epsilon = 1 / (1 + (i2\pi f\tau_{CC})^\beta) \quad (2)$$

where ϵ^* is the complex dielectric function, ϵ_∞ is dielectric constant at infinitely high frequencies, $\Delta\epsilon$ is dielectric strength, f is linear frequency, τ_{CC} is relaxation time and β is the broadening coefficient of polarization in the frequency range [18,23]. Cole-Cole fits show that increasing magnetic flux cannot change the behavior along with the whole frequency range. But also, the polarization mechanism at the lowest side of the range looks to have changed due to magnetic flux. The size of this mechanism increases by the effect of magnetic flux. However, an increase in magnetic flux cannot cause a big change among the samples under the influence of the flux. This behavior supports the results obtained from STEM images. As shown in Fig.3, the dielectric constant of PTh and PTh-4.6 are 24,6 and 82,76 at 1MHz, respectively. The reason for the difference between the dielectric constant of the samples is due to the different magnetic fields applied during the synthesis process. As seen in STEM results, the sample synthesized without a magnetic field is stiffer than the samples synthesized under a magnetic field. So, PTh-4.6 can easily keep up with the increasing frequency due to its loose aggregate and polarization increases. Thus, the dielectric constant increases [16]. The mechanism observed at frequencies higher than the former mechanism can be attributed to the polarization of the polythiophene chain. This mechanism looks affected by the magnetic flux. The increasing size of PTh nanoparticles can be the reason production of a tough structure. This structure can restrict the motion ability of chain and side chains. Thus, The Cole-Cole fits shift toward lower frequencies by the effect of the flux and with increasing flux. However, the increasing number of nanoparticles with increasing flux as observed in STEM images increases the dielectric constant due to the increasing magnitude of the polarization. The polarization mechanism at the high-frequency region ($10^5 - 10^7$ Hz) can be attributed to the polarization of side groups attached to the long polymer chain and thiophene ring. So, polarization decreases with increasing frequency, and the dielectric constant decreases [24]. At this frequency region, it looks like the increasing number of nanoparticles causes the increase of polarization and dielectric constant with the presence of the magnetic flux. Also, it can be said that the increasing flux density has a remarkable effect on the polarization of side chains.

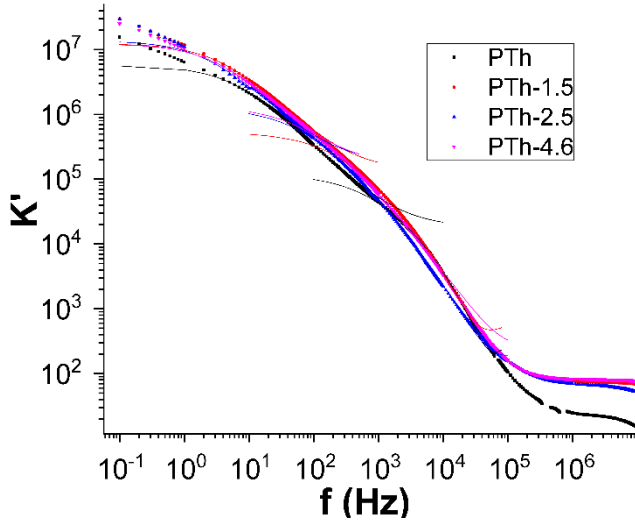


Fig. 3. Frequency dependence of dielectric constant for polythiophene nanoparticles (color online)

3.2.2. Frequency dependence of loss factor of polythiophene nanoparticles

The dielectric loss factor expresses the losses in electrical energy in the material due to nonlinear physical mechanisms such as electrical conductivity, dielectric relaxation, and dielectric resonance. These losses act as a significant thermal source at high voltage or high frequency. Since dielectric losses cause electromagnetic waves to scatter with heat, losses occurring at high frequency or high voltage act as a thermal source. This situation causes the dielectric material to be forced more heat under these conditions and affects its properties to change and may cause a decrease in the performance of dielectric materials. In material selection, the dielectric loss

factor is an important parameter in order not to see power loss and to maintain the properties of the material under operating conditions, so it is preferred that the loss factor is as small as possible when selecting dielectric materials. That's why it is also important to know how the dielectric loss factor changes under operating conditions. Relaxation times were calculated from Cole-Cole curve fits, relating $\tan \delta$ with frequency, in the following equation. Dielectric loss is a measure of the energy loss that occurs as a result of the interaction with each other and with the environment of charges trying to polarize under the effect of a variable electric field.

$$\tan \delta(\omega) = \tan \delta_{\infty} [\sin(\beta\pi/2) / (\omega\tau_0)^{-\beta} + 2\cos(\beta\pi/2) + (\omega\tau_0)^{\beta}] \quad (3)$$

The frequency dependence of the loss factor, $\tan \delta$ is shown in Fig.4. It is observed two main polarization mechanisms, which are attributed to the polarization of a PTh aggregate, a thiophene ring, and side groups, in the structure [23,25]. Also, there is an unclear mechanism described by unclear shoulders around 10^4 rad/s. These polarization mechanisms can be detected for PTh clearly while it is unable for samples which were undergone magnetic treatment because of the coinciding of two relaxation mechanisms, the relaxation mechanisms belong to PTh aggregates which are expected to observe at the low-frequency side. Where τ is relaxation time and β is a coefficient for the distribution of the relative relief over the frequency range and varies between 0 and 1 ($0 \leq \beta \leq 1$) leads to an asymmetrical broadening of the relaxation function [20]. Relaxation times are presented in Table 1 for all samples.

Table 1. The relaxation times of polythiophene nanoparticles synthesized at different magnetic fields

Sample	Magnetic flux density (k Gauss)	I.polarization region Relaxation times τ (s)	II. polarization region Relaxation times τ (s)
PTh-0	0	1.308×10^{-2}	1.773×10^{-6}
PTh-1.5	1.5	3.424×10^{-2}	3.605×10^{-6}
PTh-2.5	2.5	7.675×10^{-2}	7.392×10^{-6}
PTh-4.6	4.6	1.346×10^{-2}	3.280×10^{-6}

Relaxation times in Table 1 show that there is a big difference between the mechanisms observed on the low-frequency side and higher frequencies than the former mechanism. It looks like the mechanism which is referred to as the polarization of PTH aggregates can be interfacial polarization or space-charge polarization due to the relaxation time in the order of 10^{-2} s. The other mechanism can be attributed to the polarization of the PTh chain and it can be dipolar polarization due to the relaxation time of 10^{-6} s. The relaxation behavior which is attributed to the polarization of thiophene rings or side chains cannot be detected at the high-frequency side of the range. The results obtained in Table 1 show that lower energy loss conditions will occur if a magnetic flux density of 4.6 kGauss is applied. The results detected in Table 1 show that a magnetic flux of 4,6 kGauss in the production of these samples will ensure establishing a low energy loss using conditions in applications. The unclear mechanism can be observed clearly in section 3.2.3 by frequency-dependent AC conductivity graphs.

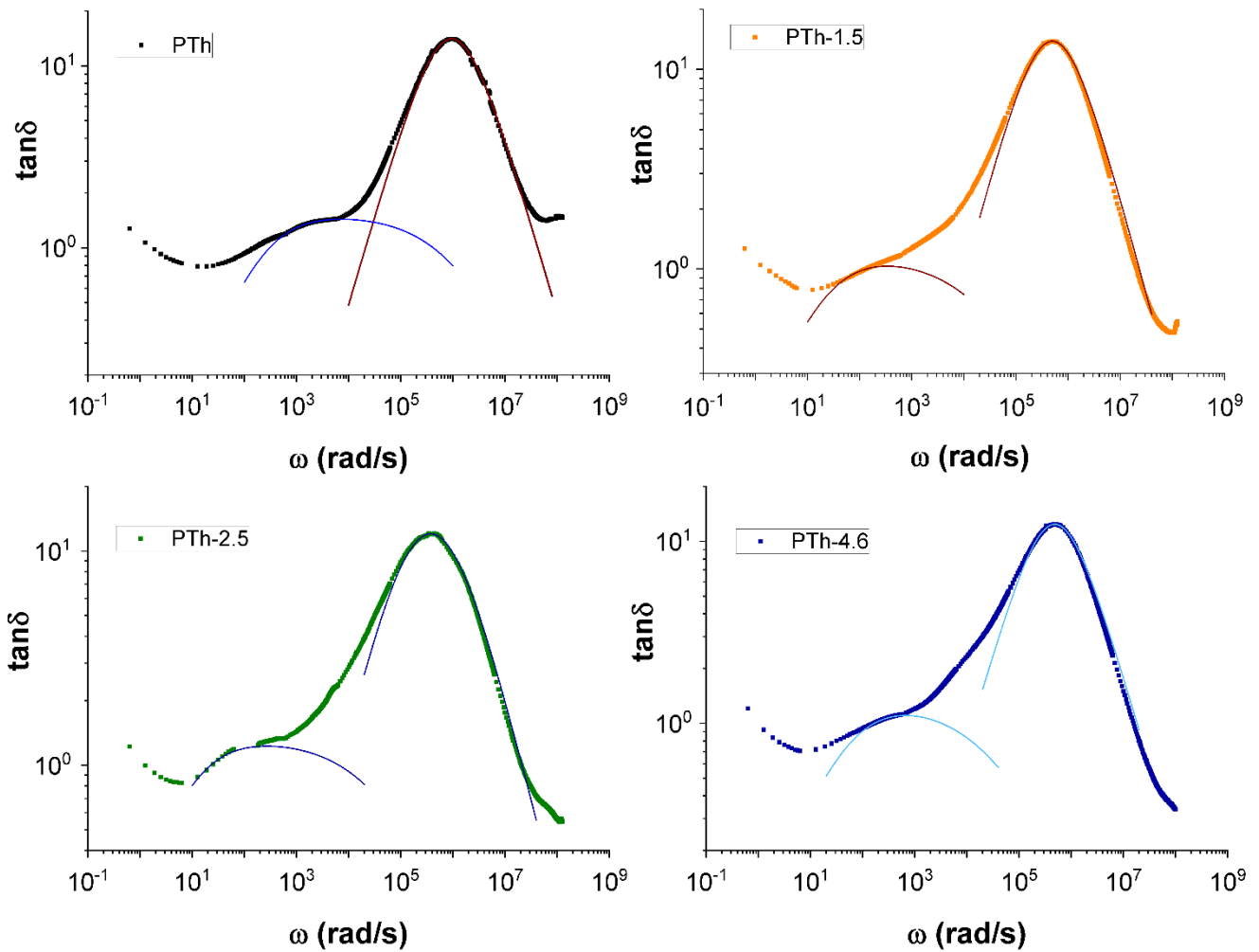


Fig. 4. Frequency dependence of loss factor, $\tan\delta$ for polythiophene nanoparticles synthesized at different magnetic fields

3.2.3. AC conductivity of polythiophene nanoparticles

The frequency dependence of the ac conductivity for PTh nanoparticles (σ_{AC}) obeys the Jonscher's Universal Dielectric Response (JUDR) [26] as given in the following equation;

$$\sigma_{AC} = \sigma_D + A\omega^s \tag{4}$$

where σ_0 , A, s are DC-like conductivity, an integer, and an exponential parameter which varies values between 0 and 1, respectively [15,17,19]. The frequency dependence of σ_{AC} at room temperature can be shown in Fig.5. Although it was interpreted that there were two polarization mechanisms detected in Fig.4 in section 3.2.2, the figure represents that polythiophene nanoparticles synthesized under different magnetic fields have three conduction mechanisms in the investigated frequency.

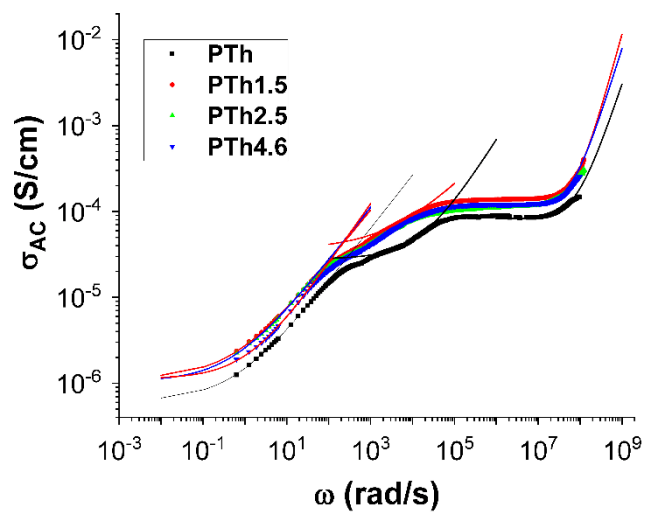


Fig. 5. Angular frequency dependence of ac conductivity, σ_{AC} for polythiophene nanoparticles synthesized at different magnetic fields

One of these mechanisms is observed in the frequency range between 10^{-1} - 10^3 rad/s which is called as first polarization mechanism and the second polarization mechanism is located at frequencies between 10^2 - 10^5 rad/s with frequency-independent AC conductivity values around 10^{-6} S/cm and $5 \cdot 10^{-5}$ S/cm, respectively. Toward frequencies higher than 10^6 rad/s, the third polarization mechanism is detected with frequency-independent AC conductivity values around 10^{-4} S/cm [27]. The first polarization mechanism may be attributed to the polarization of the long polymer chain while the second polarization mechanism can be attributed to the polarization of the thiophene ring. The third polarization mechanism can be attributed to the polarization of side groups [15,18,28–32].

4. Conclusions

Polythiophene nanoparticles successfully synthesized without a magnetic field and with different magnetic flux densities of 1.5, 2.5, and 4.6 k Gauss were studied. The STEM images revealed that magnetic fields considerably affect the aggregation of polythiophene chains and consequently the morphology of the nanoparticles. Results on frequency and temperature dependence of dielectric constant, K' and loss factor, and $\tan\delta$ of polythiophene nanoparticles are presented. These parameters decrease with increasing frequency at room temperature. For all samples, the polarization mechanisms and relaxation times were determined by using the Cole-Cole equation. All samples exhibit three polarization mechanisms according to ac conductivity results. Consequently, this work provides new information about the dielectric characterization and structure of polythiophene nanoparticles synthesized at different magnetic fields to use in electronic devices and the microelectronic industry. The results obtained in Table 1 show that lower energy loss conditions will occur if a magnetic flux density of 4.6 kGauss is applied. The results detected in Table 1 show that a magnetic flux of 4,6 kGauss in the production of these samples will ensure establishing a low energy loss using conditions in applications.

Acknowledgments

This study was partially supported by the Scientific Research Project Coordination of Yildiz Technical University (Project numbers: 2016-01-02-DOP02 and 2015-01-02-KAP02) and the Department of Scientific Research Projects of Istanbul University (I.U. BAP) [grant numbers 7364, and 30048].

References

- [1] F. Vatansever, J. Hacaloglu, U. Akbulut, L. Toppare, *Polym. Int.* **41**(3), 237 (1996).
- [2] D. C. Tiwari, V. Sen, R. Sharma, *Indian J. Pure Appl. Phys.* **50**, 49 (2012).
- [3] S. Sakthivel, A. Boopathi, *Int. J. Sci. Res.* **141**, 97 (2014).
- [4] M. Okutan, Y. Yerli, S. E. San, F. Yilmaz, O. Günaydin, M. Durak, *Synth. Met.* **157**(8–9), 368 (2007).
- [5] A. Laforgue, P. Simon, C. Sarrazin, J. F. Fauvarque, *J. Power Sources* **80**(1), 142 (1999).
- [6] M. R. Karim, C. J. Lee, M. S. Lee, *J. Polym. Sci. Part A Polym. Chem.* **44**(18), 5283 (2006).
- [7] R. S. Bobade, *J. Polym. Eng.* **31**(2–3), 209 (2011).
- [8] K. M. Molapo, P. M. Ndingili, R. F. Ajayi, G. Mbambisa, S. M. Mailu, N. Njomo, M. Masikini, P. Baker, E. I. Iwuoha, *Int. J. Electrochem. Sci.* **7**, 11859 (2012).
- [9] J. Kattimani, T. Sankarappa, K. Praveenkumar, J. S. Ashwajeet, C. G. B, T. Sujatha, *Int. J. Adv. Res. Phys. Sci.* **1**(7), 17 (2014).
- [10] K. Majid, R. Tabassum, A. F. Shah, S. Ahmad, M. L. Singla, *J. Mater. Sci. Mater. Electron.* **20**(10), 958 (2009).
- [11] S. V Kamat, S. H. Tamboli, V. Puri, R. K. Puri, J. B. Yadav, S. Joo, *J. Optoelectron. Adv. M.* **12**(11), 2301 (2010).
- [12] S. Kamat, S. H. Tamboli, V. Puri, R. K. Puri, O. Shom Joo, *Arch. Phys. Res.* **1**(4), 119 (2010).
- [13] O. Y. Gumus, H. I. Unal, O. Erol, B. Sari, *Polym. Compos.* **32**(3), 418 (2011).
- [14] K. Huner, F. Karaman, *Mater. Res. Express* **6**(015302), 1 (2019).
- [15] S. Yakut, K. Ulutas, D. Deger, *Thin Solid Films* **645**, 269 (2018).
- [16] S. Yakut, H. K. Ulutas, I. Melnichuk, A. Choukourov, H. Biederman, D. Deger, *Thin Solid Films* **616**, 279 (2016).
- [17] S. Yakut, K. Ulutaş, D. Bozoglu, M. Adibelli, T. Ceper, N. Arsu, D. Deger, *Phys. B Condens. Matter* **542**, 6 (2018).
- [18] S. Yakut, K. Ulutas, D. Deger, *Mater. Sci. Eng. C* **104**(109962), 1 (2019).
- [19] Ş. Yakut, *J. Fac. Eng. Archit. Gazi Univ.* **36**(2), 1105 (2021).
- [20] F. Kremer, S. Andreas, *Broadband Dielectric Spectroscopy*, Springer-Verlag Berlin Heidelberg, New York (2003).
- [21] M. Parto, D. Deger, K. Ulutas, S. Yakut, *Appl. Phys. A Mater. Sci. Process.* **112**(4), 911 (2013).
- [22] S. B. Aziz, O. G. Abdullah, S. R. Saeed, H. M. Ahmed, *Int. J. Electrochem. Sci.* **13**(4), 3812 (2018).
- [23] A. R. Von Hippel, *Dielectrics and Waves*, Ed. by New York, Wiley; London, Chapman & Hall (1954).
- [24] M. Ajmal, M. U. Islam, A. Ali, *J. Supercond. Nov. Magn.* **31**(5), 1375 (2018).
- [25] H. Rekik, Z. Ghallabi, I. Royaud, M. Arous, G. Seytre, G. Boiteux, A. Kallel, *Compos. Part B Eng.* **45**(1), 1199 (2013).
- [26] A. K. Jonscher, *Nature* **267**(5613), 673 (1977).
- [27] K. Shehzad, Z. M. Dang, M. N. Ahmad, R. U. R. Sagar, S. Butt, M. U. Farooq, T. B. Wang, *Carbon N. Y.* **54**, 105 (2013).

- [28] A. Roy, K. Prasad, A. Prasad, *Process. Appl. Ceram.* **7**(2), 81 (2013).
- [29] S. Diaham, M.L. Locatelli, T. Lebey, S. Dinculescu, *EPJ Appl. Phys.* **49**(10401), 1 (2010).
- [30] M. S. Graff, R. H. Boyd, *Polymer* **35**(9), 1797 (1994).
- [31] M. Serin, D. Sakar, H. Cankurtaran, O. Cankurtaran, F. Karaman, *J. Optoelectron. Adv. M.* **7**(6), 3121 (2005).
- [32] M. Serin, D. Sakar, O. Cankurtaran, F. Karaman, *J. Optoelectron. Adv. M.* **8**(3), 1308(2006).

*Corresponding authors: serin@yildiz.edu.tr;
yakuts@istanbul.edu.tr